8B.5 A QUASI-OBJECTIVE METHOD FOR DISCRIMINATION OF SUPERCELL ARCHETYPES USING THE WSR-88D

Kyle A. Beatty*, University of Oklahoma
J. M. Straka, E. N. Rasmussen, and L. R. Lemon

1. INTRODUCTION

Several refereed and non-refereed papers (e.g., Doswell and Przybylinski 1990; Doswell and Burgess 1993; Moller et al. 1994; Rasmussen and Straka 1998) have described the characteristics of supercell precipitation variants. Each of these publications has provided anecdotal evidence that a storm's severity is related to the amount and spatial distribution of its precipitation. Supercells have most often been described in the archetypical classes of low precipitation (LP), classic, and high precipitation (HP) supercells.

The methods used by individuals to characterize a supercell's precipitation distribution often vary. The most common tools used are weather radar (reflectivity in particular) and visual observation. Distinguishing between which method is used to characterize a storm's precipitation distribution is critical. At large ranges, a storm may appear to have substantial precipitation in its left and rear flanks on radar because the storm is being sampled at mid levels. In actuality, there may not be any hydrometeors in this region below the radar horizon. Alternatively, large raindrops of low concentration often do not significantly attenuate light and therefore may not be visible to the eye, but would have substantial reflectivity on radar due to the large dependence of reflectivity Z on hydrometeor diameter D (e.g., $Z \propto D^6$). Therefore a storm that may appear to have no precipitation in its left or rear flanks may actually have highly reflective hydrometeors in its rear flank downdraft that give it a classical radar appearance. For example, to our knowledge, only a few cases of "true" LP supercells (i.e., those void of precipitation in left and rear flanks of the updraft; Rasmussen and Straka 1998) have been documented (e.g., Davies-Jones et al. 1976).

* Corresponding author address: Kyle A. Beatty, Risk Management Solutions, Inc., 7015 Gateway Blvd., Newark, CA, 94560; e-mail: kyle.beatty@rms.com.

In this paper, we propose a quasi-objective method to systematically evaluate supercell precipitation characteristics based on the spatial relationship between the radar-inferred precipitation core and the supercell updraft. The analysis of a sample of supercells indicates the potential to objectively discriminate between supercells based on their reflectivity mode, which is defined by the updraft-relative position of the reflectivity centroid. We suggest that this or a similar method be used in further research to quantify the relationship between precipitation characteristics and storm severity.

2. DATA AND METHODS OF ANALYSIS

The seven cases that were evaluated are listed in Table 1. In each case, reported visual-based archetypes are noted as well as the storm's reflectivity mode. Each storm's supercell phase was defined as the period with a persistent mesocyclone radar signature at mid levels. The analysis period for each case was further constrained to a distance of 30 to 125 km from the radar. This range criterion was used to limit the center radar beam height to 2.0 km and to ensure sufficient vertical scans to identify features indicative of the supercell updraft.

TABLE 1: SAMPLE OF SUPERCELL CASES STUDIED

Name/Date (mm/dd/yy)	Radar Vols	Visual Archetype /Reflectivity Mode
Plainview, TX 05/25/94	12	unknown/Forward
Okla. Storm A 05/03/99	11	CL/Forward
Okla. Storm B 05/03/99	32	LP-CL/Forward
Guthrie, OK 06/13/98	15	LP/Forward
Oklahoma City, 06/13/98	18	CL/Forward
Near Lubbock, TX 05/25/99	11	HP/Rear
Kaw Reservoir, OK 05/06/94	45	HP/Rear

For each case, the lowest elevation of the WSR-88D radar (0.5º elevation) was used to estimate the location of the near-surface precipitation core. A closed polygon was defined around the supercell echo at this level of each volume

during the supercell's existence through use of an adapted version of the Map 1.02 software application, developed by Erik Rasmussen (2003). An example of the bounding polygon identified for a scan of the May 25, 1999 supercell near Lubbock is shown in Figure 1 on page 4. When a supercell is not isolated, the boundary of the supercell echo was estimated subjectively by identifying and excluding individual cells that merge with or propagate away from the supercell echo. The rain rate centroid R_c is estimated within the closed polygon assuming the *Z*-*R* relation

$$Z = 0.01 * R^{0.833} \text{ where } 10 \le Z \le 53$$

The conservative threshold of *Z* values in excess of 10 dBZ was used to exclude values that may be associated with index-of-refraction variations in the air rather than the cloud/precipitation field (Knight and Miller 1993). Reflectivity *Z* is truncated at 53 dBZ to reduce the hail bias in rain rate estimation (Vieux and Bedient 1998). The formulae used to calculate the centroid components R_{cx} and R_{cy} are

$$R_{cx} = \frac{\sum_{i=1}^{n} (X_i * R_i)}{\sum_{i=1}^{n} R_i}; R_{cy} = \frac{\sum_{i=1}^{n} (Y_i * R_i)}{\sum_{i=1}^{n} R_i}$$

Prior to the identification of features indicative of the supercell updraft, the coordinates of the radar sample volumes were adjusted to remove the translation of echo associated with storm motion between elevation scans. Removal of this component of motion is important to properly estimate the tilt of the updraft axis, for later extrapolation to lower levels. The coordinates of R_{cx} and R_{cy} were also adjusted to maintain a consistent reference frame. A conceptual diagram of the location of the rain rate centroid relative to the extrapolated position of the low-level updraft is shown in Figure 2 on page 4.

The approximate axis of peak updraft velocity was subjectively identified at two or more elevation angles per radar volume (e.g., following Lemon 1980; Lemon 1998). The detection of a bounded weak echo region (BWER; also known as a vault) in the mid-levels of a thunderstorm was considered a sufficient (but not a necessary) condition for the identification of an organized updraft (Marwitz et al. 1972; Browning 1978). Assuming updraft linearity, the area of concavity that is bordered by the maximum reflectivity gradient in the lower levels of the storm and the echo summit/area of maximum summit divergence aloft were also used to identify points along the updraft axis. Since these features were not identifiable at all ranges or stages within a supercell's life cycle, the four-dimensional radar presentation was considered for all three radar moments to establish time and height continuity of the estimated updraft axis. The coordinates of the low-level updraft location are estimated at 1.15 km above radar level (midpoint of range domain) using least squares linear regression of the mid- and upper-level updraft centers. The distance between the estimated low-level updraft location and R_c, as well as the location of R_c relative to ***c*** were then determined.

3. CONCLUSIONS AND DISCUSSION

Despite its simplicity, the location of the rain rate centroid relative to the storm motion vector seems to be a fairly robust method to distinguish between storms with classical/LP and those with HP visual appearances (Fig. 3). The classic and LP storms have a low-level rain rate centroid in their forward flanks, while the HP storms have a low-level rain rate centroid in their rear flanks. This finding is intuitive and consistent with the description of HP supercells in past literature, which often evolve from the classic to HP state with the development and maintenance of a strong RFD and an associated increased amount of precipitation on the rear side of the updraft. The findings from this sample indicate that there may be two dominant reflectivity modes, whereby storms maintain precipitation either in the front or rear flanks. It is possible that "true" LP storms that have no precipitation in their rear flanks might have greater distances between their low level updraft and rain rate centroid that would make these storms distinct. In this case set, while some storms were described to appear as LP, all had significant reflectivity to the left and rear of their updrafts indicating a classic radar appearance. For example, storms A and B on 13 June 1998 had very different visual appearances, but were very similar when viewed by radar.

Based on this research, we recommend that precipitation classification of supercells be done

consistently via radar when the storm is within sufficient range and not via visual appearance. Visual appearances are subjective and therefore frequently lead to conflicting conclusions. In doing so, we suggest using the terms **"forward reflectivity mode (Forward)"** and **"rear reflectivity mode (Rear)"** to distinguish between supercells viewed on radar. We further suggest that this quasi-objective approach for characterizing supercell precipitation variants be applied consistently to a larger sample of storms to support or refute anecdotal evidence of favored degrees of severity within different archetypes. This approach could also be used to evaluate environmental forcing mechanisms with an objective basis for determining storm precipitation characteristics, with the potential for anticipating reflectivity mode in the forecast and storm warning processes.

If supporting data are available, future calibration of the *Z-R* relationship may provide further improvements in the analysis technique. Finally, although not critical in this case set, in a larger sample it would be necessary to stratify results by storm depth, since storms that are shallower will inherently have shorter separation distances because of their smaller spatial scale.

4. ACKNOWLEDGEMENTS

The thesis form which this work was derived was financially supported in part by a Graduate Fellowship from the American Meteorological Society and a grant from the National Science Foundation. We would also like to thank Lou Wicker of the National Severe Storms Laboratory for his temporary funding in this effort. Data used in this study were provided by the National Climatic Data Center.

5. REFERENCES

Doswell, C. A. III, and R. Przybylinski, 1990: A unified set of conceptual models for variations on the supercell theme. *Preprints, 16th Conf. Severe Local Storms*, Kananaskis Park, Alberta, Amer. Meteor. Soc., 40-45.

____, and D. W. Burgess, 1993: Tornadoes and tornadic storms: A review of conceptual models. *The Tornado: Its Structure, Dynamics, Prediction, and Hazards*, Geophys. Monogr., Amer. Geophys. Union, 161-172.

Browning, K. A., 1978: The structure and mechanisms of hailstorms. *Hail: A Review of Hail Science and Suppression*, G. Foote and C. Knight, Eds., *Meteor. Monogr.*, No. 38, Amer. Meteor. Soc., 1-43.

Davies-Jones, R. P., D. W. Burgess, and L. R. Lemon, 1976: An atypical tornado-producing cumulonimbus. *Weather*, **31**, 336-347.

Knight, C. A., and L. J. Miller, 1993: First radar echoes from cumulus clouds. *Bul. Amer. Meteor. Soc.*, **74**, 179-188.

Lemon, L.R., 1980: Severe thunderstorm radar identification techniques and warning criteria. NOAA Tech. Memo. NWS NSSFC-3, 60 pp.

_____, 1998: Updraft identification with radar. *Preprints, 19th Conf. Severe Local Storms*, Minneapolis, Amer. Meteor. Soc., 709-712.

Marwitz, J. D., 1972a: The structure and motion of severe hailstorms. Part III: Severely sheared storms. *J. Appl. Meteor.*, **11**, 189-201.

Moller, A. R., M. P. Foster, and G. R. Woodall, 1994: The operational recognition of supercell thunderstorm environments and storm structures. *Wea. Forecasting*, **9**, 327-347.

Rasmussen, E. N., 2003: *Map 3D Visualization Package, Explanations and Tutorials*. http://www.nssl.noaa.gov/ssr/.

____, and J. M. Straka, 1998: Variations in supercell morphology. Part I: Observations of the role of upper-level storm-relative flow. *Mon. Wea. Rev.*, **126**, 2406-2421.

Vieux, B.E., and P.B. Bedient, 1998: Estimation of Rainfall for Flood Prediction from WSR-88D Reflectivity: A Case Study, 17-18 October 1994. *Wea. Forecasting*, **13**, 126-134

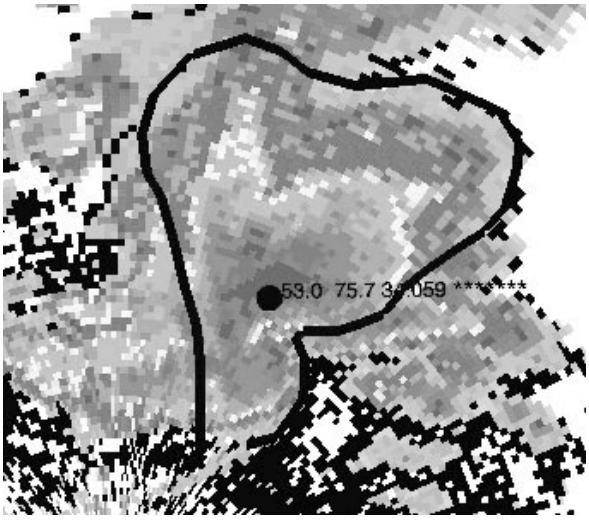

Figure 1: Example of the polygon defined to bound the storm and the rain rate centroid within this area for a scan of the May 25, 1999 supercell located immediately northwest of the Lubbock radar (KLBB).

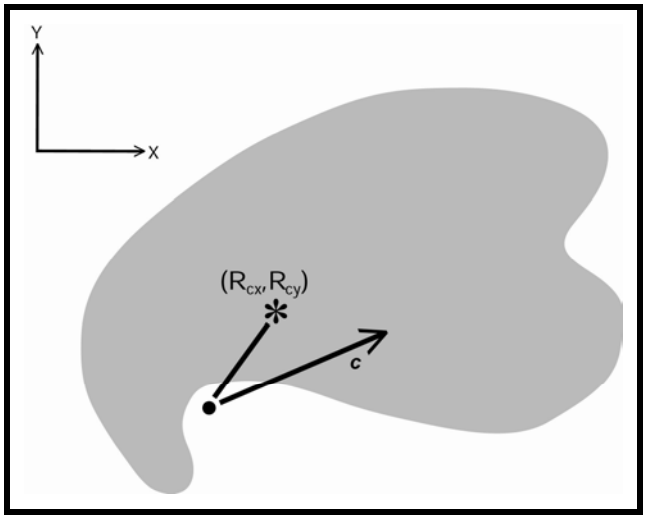

Figure 2: Conceptual illustration of the rain rate centroid relative to the storm motion vector. View is of the x-y plane. The black dot represents the extrapolated position of the supercell updraft at the map height. The asterisk represents the location of the rain rate centroid.

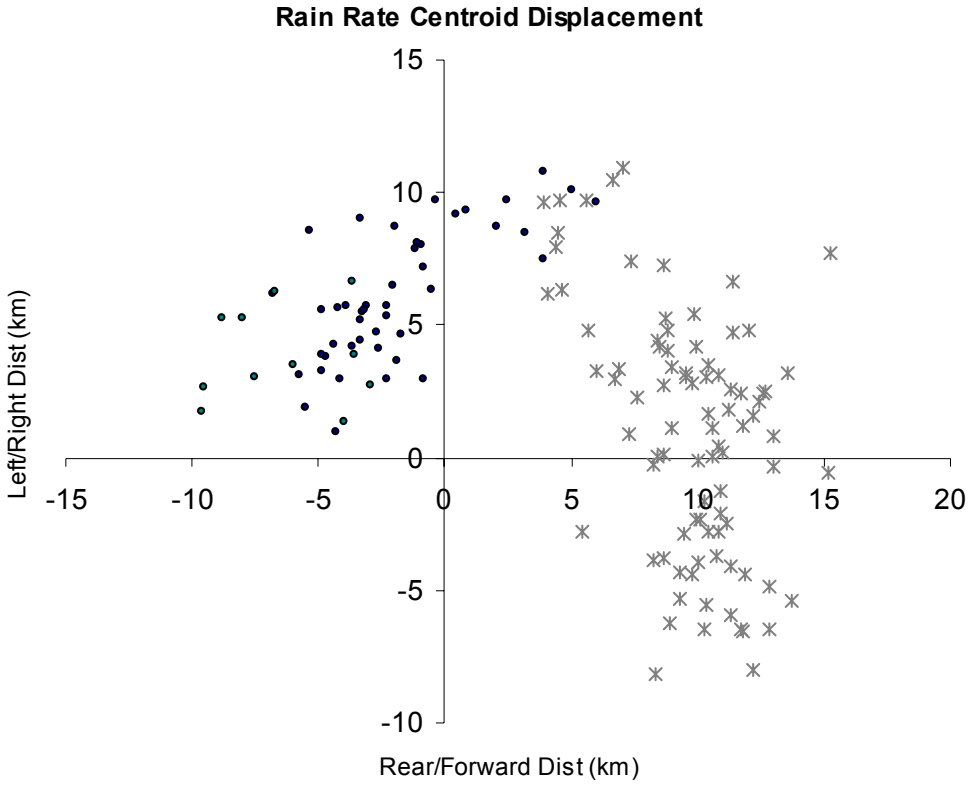

Figure 3: Updraft relative rain rate centroid locations for all cases. Data has been adjusted to a common frame, with storm motion from left to right. Storms with an HP radar appearance are shown as black dots, while those with classical radar appearances are shown as crosses in grey.